DESIGN OF CONTROL FOR A SERIAL ROBOT WITH ACTUATOR FAILURES

Le Ngoc TRUC[1], Nguyen Phung QUANG[2]

The paper addresses the actuator failure issue and aims to design a satisfactory control scheme for an n-DOF serial robot under actuator failures. The kind of actuator failures that is put into investigation in this study is the proportional degradation of actuator torque. A sliding mode controller using adaptive techniques is developed to deal with the faults. The switching gains of the proposed controller are alterable and can be suitably regulated to satisfy the Lyapunov criterion. The effectiveness of the proposal control law applied for a 6-DOF serial robot is shown through comparison with a conventional sliding mode controller.

Keywords: Sliding Mode Control, Adaptive Control, Robotic System, Actuator Fault, Manipulator, Serial Robot.

1. Introduction

Robots have been used in various applications and places because of their undeniable pre-eminent abilities [1], [2]. Presently, due to the increasing demand for the utilization of robots in production chains and/or in dangerous environments, the robot's fault-tolerant ability has received significant attention. A robot system will commonly respond to failures by stopping the whole system. The downtime caused by the repair or replacement of faulty parts can affect productivity and manufacturing efficiency. Through an investigation of failures in industrial robots, the general failures can be detected by criteria of training data [3]. Many researches showed that some faulty types in a robot could be accommodated by suitable strategies. One of these fault types is the unwanted reduction of the actuator torque, which is considered in this study. The faulty actuator may be kept operating, or be put into a safe-mode to avoid unnecessary damages. In general, investigation topics related to actuator faults are detection, location, diagnosis, and fault-tolerant control design. Numerous contributions regarding to the first three topics are presented. Some approaches used Support-Vector-Machines [4] or a partial-least-squares based statistical theory [5] to detect

[1] Faculty, Hung Yen University of Technology and Education, Vietnam; Researcher, Hanoi University of Science and Technology, Vietnam, e-mail: lengoc.truc@utehy.edu.vn (corresponding author)
[2] Prof., Institute for Control Engineering and Automation, Hanoi University of Science and Technology, Vietnam, e-mail: quang.nguyenphung@hust.edu.vn

and to locate the robot actuator faults. To identify failures in robot actuators, a nonlinear observer based on the robot dynamics [6] and a fault identification scheme using a linear robust observer of fault time profiles [7] are proposed. In [8], a discrete-time framework processed by a decision-making system for fault diagnosis is devised. An adaptive fault diagnosis for multiple actuators and sensors is provided in [9]. The robot behavior is analyzed in case of a single free-swinging joint [10], a single locked joint with trajectory planning [11], and actuator torque degradation [12].

For the last topic: the design of fault-tolerant controllers, several approaches have been proposed. In [13], an embedded adaptation scheme is synthesized to compensate the torque degradation and to maintain the robot performance. An adaptive fault-tolerant control based on boundary estimation is designed for a space robot under partial loss of actuator effectiveness [14]. The study in [15] presents an adaptive control using a backstepping design for robot manipulators with joint constraints and actuator failures. Sliding mode based techniques have been used widely in many fields of investigation [16], [17]; and there is also not excluded in the field of robot control. A reconstruction for robot actuator faults is developed by using terminal sliding mode fashion [18]. To overcome the fault of additive time-varying and constant torque, a fault-tolerant control based on the sliding mode technique for robotic arms is provided in [19]. Various researches that deal with the combination of actuator fault detection, analysis, and control are: [20] for flexible-joint robots, [21] for robots with free-swinging joints, and [22] for SSRMS-type manipulators with locked joints. Motivated by the above results, the paper presents a sliding mode controller using adaptive parameters to deal with actuator failures existing in a 6-DOF serial robot. The considered fault type of actuators is the proportional degradation of torque. The parameters of the proposed sliding mode controller are regulated or changed by an adaptive law satisfying the Lyapunov-based system stability. The degradation of actuator torque can be tolerated with acceptable responses under reasonable levels of faults. The structure of this paper is as follows. Section 2 provides the dynamic model of a serial robot and the problem of the degradation of actuator torque. Section 3 presents the design of a fault-tolerant controller. In section 4, the efficiency of the proposed controller is shown through simulation and comparison with another controller. Finally, section 5 states the conclusion of this study.

2. System model and problem statement

Let us consider an n-DOF robot dynamic model without friction as

$$\mathbf{M}\ddot{\mathbf{q}} + \mathbf{C}\dot{\mathbf{q}} + \mathbf{g} = \boldsymbol{\tau}_a \tag{1}$$

where $\mathbf{q} \in \mathbb{R}^n$ is the joint variable, $\boldsymbol{\tau}_a \in \mathbb{R}^n$ is the actual torque generated by actuators, $\mathbf{M} \coloneqq \mathbf{M}(\mathbf{q}) \in \mathbb{R}^{n\times n}$ is the generalized inertia matrix, $\mathbf{C} \coloneqq \mathbf{C}(\mathbf{q}, \dot{\mathbf{q}}) \in \mathbb{R}^{n\times n}$ is the Coriolis/centrifugal matrix, $\mathbf{g} \coloneqq \mathbf{g}(\mathbf{q}) \in \mathbb{R}^n$ is the gravity term. Robot actuators are subjected to be the fault type: Proportional Degradation of Torque (PDT), where the actuator torque $\boldsymbol{\tau}_a$ can be replaced by

$$\boldsymbol{\tau}_a = \boldsymbol{\Phi}\boldsymbol{\tau}_c \tag{2}$$

where $\boldsymbol{\tau}_c$ is the control torque, $\boldsymbol{\Phi} = \mathrm{diag}(\boldsymbol{\varphi})$ is the n-by-n diagonal matrix, $\boldsymbol{\varphi} = [\varphi_1, \varphi_2, \dots, \varphi_n]^T$ is the torque degradation coefficient vector, $\varphi_i \in [0,1]$, $i = 1, 2, \dots, n$. Actuator i has either no torque fault if $\varphi_i = 1$ or a PDT fault if $0 < \varphi_i < 1$. Especially, if $\varphi_i = 0$, the torque of actuator i will be the total loss and joint i becomes free-swinging. Because the generalized inertia matrix $\mathbf{M}$ is positive definite and invertible, the dynamic equation (1) can be written as

$$\ddot{\mathbf{q}} = -\mathbf{M}^{-1}(\mathbf{C}\dot{\mathbf{q}} + \mathbf{g}) + \mathbf{M}^{-1}\boldsymbol{\Phi}\boldsymbol{\tau}_c \tag{3}$$

or by the compact form:

$$\ddot{\mathbf{q}} = \mathbf{f} + \mathbf{B}\boldsymbol{\tau}_c \tag{4}$$

where

$$\mathbf{f} \coloneqq -\mathbf{M}^{-1}(\mathbf{C}\dot{\mathbf{q}} + \mathbf{g}), \quad \mathbf{B} = \mathbf{M}^{-1}\boldsymbol{\Phi} \tag{5}$$

Due to $\mathbf{M}$, $\mathbf{C}$, $\mathbf{g}$, and $\boldsymbol{\Phi}$ are not known perfectly, $\mathbf{f}$ and $\mathbf{B}$ are also not known precisely. But we can have $\mathbf{f} = \hat{\mathbf{f}} + \tilde{\mathbf{f}}$ and $\mathbf{B} = \widehat{\mathbf{B}} + \widetilde{\mathbf{B}}$ where $\hat{\mathbf{f}}$ and $\widehat{\mathbf{B}}$ are the nominal values of $\mathbf{f}$ and $\mathbf{B}$, respectively. The estimation errors $\tilde{\mathbf{f}}$, $\widetilde{\mathbf{B}}$ are assumed to be the matched uncertainties. In the next section, with the desired joint trajectory $\mathbf{q}_d \in \mathbb{R}^n$ and under the presence of uncertainties, an adaptive sliding mode controller is designed to steer $\mathbf{q}$ to $\mathbf{q}_d$ and make the tracking error $\mathbf{e} = \mathbf{q}_d - \mathbf{q}$ convergent to zero.

3. Adaptive sliding mode controller for anticipating PDT faults

Commonly, the robustness of sliding mode control will be achieved by the proper choice of switching gains if the system uncertainties are constrained and their bounds are known. However, the bounds of system uncertainties are mostly unknown in practice. Therefore, an adaptive law will be used to adjust the controller parameters. The sliding manifold $\mathbf{s} = [s_1, s_2, \dots, s_n]^T$ is chosen as

$$\mathbf{s} = \mathbf{A}\mathbf{e} + \dot{\mathbf{e}} \tag{6}$$

where $\mathbf{A} = \mathrm{diag}(\boldsymbol{\alpha})$ is the n-by-n diagonal matrix with $\boldsymbol{\alpha} = [\alpha_1, \alpha_2, \dots, \alpha_n]^T$, $\alpha_i > 0$ $(i = 1, 2, \dots, n)$ is chosen such that sliding surface $s_i = \alpha_i e_i + \dot{e}_i$ has stable dynamics. Taking the time derivative of (6) yields

$$\begin{aligned}\dot{\mathbf{s}} &= \mathbf{A}\dot{\mathbf{e}} + \ddot{\mathbf{e}} = \mathbf{A}\dot{\mathbf{e}} + \ddot{\mathbf{q}}_d - \ddot{\mathbf{q}} \\ &= \mathbf{A}\dot{\mathbf{e}} + \ddot{\mathbf{q}}_d - (\mathbf{f} + \mathbf{B}\boldsymbol{\tau}_c) \\ &= \mathbf{A}\dot{\mathbf{e}} + \ddot{\mathbf{q}}_d - (\hat{\mathbf{f}} + \tilde{\mathbf{f}} + (\hat{\mathbf{B}} + \tilde{\mathbf{B}})\boldsymbol{\tau}_c) \\ &= \mathbf{A}\dot{\mathbf{e}} + \ddot{\mathbf{q}}_d - (\hat{\mathbf{f}} + \hat{\mathbf{B}}\boldsymbol{\tau}_c) - (\tilde{\mathbf{f}} + \tilde{\mathbf{B}}\boldsymbol{\tau}_c)\end{aligned} \tag{7}$$

The total loss of actuator torque is not considered in this study. Coefficient $\boldsymbol{\varphi} > 0$ therefore $\boldsymbol{\Phi}$, $\mathbf{B}$, and $\widehat{\mathbf{B}}$ are invertible. The adaptive sliding mode control law has the following form

$$\begin{aligned}\boldsymbol{\tau}_c &= \boldsymbol{\tau}_{no} + \boldsymbol{\tau}_{dis} \\ \boldsymbol{\tau}_{no} &= \hat{\mathbf{B}}^{-1}(\mathbf{A}\dot{\mathbf{e}} + \ddot{\mathbf{q}}_d - \hat{\mathbf{f}}) \\ \boldsymbol{\tau}_{dis} &= \hat{\mathbf{B}}^{-1}\hat{\boldsymbol{\Psi}}\,\mathrm{sgn}(\mathbf{s})\end{aligned} \tag{8}$$

where $\boldsymbol{\tau}_{no}$ is the nominal control term, $\boldsymbol{\tau}_{dis}$ is the adaptive discontinuous control term, $\widehat{\boldsymbol{\Psi}} = \mathrm{diag}(\widehat{\boldsymbol{\psi}})$ is the n-by-n diagonal matrix with $\widehat{\boldsymbol{\psi}} = [\hat{\psi}_1, \hat{\psi}_2, \dots, \hat{\psi}_n]^T$ being the adjustable constant vector, $\mathrm{sgn}(\mathbf{s}) \coloneqq [\mathrm{sgn}(s_1), \mathrm{sgn}(s_2), \dots, \mathrm{sgn}(s_n)]^T$ is the vector of sign function $\mathrm{sgn}(s_i)$ defined as

$$\mathrm{sgn}(s_i) = \begin{cases} 1 & \text{if } s_i > 0 \\ 0 & \text{if } s_i = 0 \\ -1 & \text{if } s_i < 0 \end{cases} \tag{9}$$

Substituting (8) into (7) gives

$$\begin{aligned}\dot{\mathbf{s}} &= \mathbf{A}\dot{\mathbf{e}} + \ddot{\mathbf{q}}_d - (\hat{\mathbf{f}} + \hat{\mathbf{B}}\boldsymbol{\tau}_c) - (\tilde{\mathbf{f}} + \tilde{\mathbf{B}}\boldsymbol{\tau}_c) \\ &= -\hat{\boldsymbol{\Psi}}\,\mathrm{sgn}(\mathbf{s}) - \mathbf{p}\end{aligned} \tag{10}$$

where $\mathbf{p} \coloneqq \tilde{\mathbf{f}} + \tilde{\mathbf{B}}\boldsymbol{\tau}_c = [p_1, p_2, \dots, p_n]^T$ is the combined uncertain vector. It is an assumption that there exists a constant vector $\boldsymbol{\psi} = [\psi_1, \psi_2, \dots, \psi_n]^T$ satisfying $\psi_i > |p_i|$, $i = 1, 2, \dots, n$. Therefore, if an adaptive law can adjust $\widehat{\boldsymbol{\Psi}}$ convergent to $\boldsymbol{\Psi} = \mathrm{diag}(\boldsymbol{\psi})$, every one-by-one element of $\dot{\mathbf{s}}$ will have opposite sign with that of $\mathbf{s}$. We define the adaptive law as

$$\begin{aligned}\dot{\hat{\psi}}_i &= \delta_i |s_i| \\ &= \delta_i s_i\,\mathrm{sgn}(s_i)\end{aligned} \tag{11}$$

where $\delta_i > 0$ $(i = 1, 2, \dots, n)$ is the chosen positive coefficient. The adaptation speed is determined by δ_i. The larger δ_i, the faster matching convergence. The adaptation error matrix and vector are $\widetilde{\boldsymbol{\Psi}} = \boldsymbol{\Psi} - \widehat{\boldsymbol{\Psi}}$ and $\widetilde{\boldsymbol{\psi}} = \boldsymbol{\psi} - \widehat{\boldsymbol{\psi}}$, respectively. Let us choose a vector-type of Lyapunov function candidates as

$$\mathbf{V} = \frac{1}{2}\mathbf{S}\mathbf{s} + \frac{1}{2}\boldsymbol{\Delta}^{-1}\widetilde{\boldsymbol{\Psi}}\widetilde{\boldsymbol{\psi}} \tag{12}$$

where $\mathbf{S} = \text{diag}(\mathbf{s})$ and $\mathbf{\Delta} = \text{diag}(\boldsymbol{\delta})$ are the n-by-n diagonal matrices, $\boldsymbol{\delta} = [\delta_1, \delta_2, \dots, \delta_n]^T$, $\mathbf{\Delta}^{-1} = \text{diag}([\delta_1^{-1}, \delta_2^{-1}, \dots, \delta_n^{-1}]^T) > 0$ is the inverse matrix of $\mathbf{\Delta}$, and $V_i = \frac{1}{2}s_i^2 + \frac{1}{2}\delta_i^{-1}\tilde{\psi}_i^2 > 0$ is the ith Lyapunov function candidate. Taking the time derivative of $\mathbf{V}$ obtains

$$\dot{\mathbf{V}} = \mathbf{S}\dot{\mathbf{s}} + \mathbf{\Delta}^{-1}\tilde{\mathbf{\Psi}}\dot{\tilde{\boldsymbol{\psi}}} \tag{13}$$

After inserting (10) into (13) we obtain

$$\dot{\mathbf{V}} = \mathbf{S}(-\hat{\mathbf{\Psi}}\,\text{sgn}(\mathbf{s}) - \mathbf{p}) + \mathbf{\Delta}^{-1}\tilde{\mathbf{\Psi}}\dot{\tilde{\boldsymbol{\psi}}} \tag{14}$$

Because $\boldsymbol{\psi}$ is a constant vector, therefore $\dot{\tilde{\boldsymbol{\psi}}} = -\dot{\hat{\boldsymbol{\psi}}}$ and deduce

$$\dot{\mathbf{V}} = -\mathbf{S}\hat{\mathbf{\Psi}}\,\text{sgn}(\mathbf{s}) - \mathbf{S}\mathbf{p} - \mathbf{\Delta}^{-1}(\mathbf{\Psi} - \hat{\mathbf{\Psi}})\dot{\hat{\boldsymbol{\psi}}} \tag{15}$$

From the adaptive law (11) we have

$$\dot{\hat{\boldsymbol{\psi}}} = \mathbf{\Delta}\mathbf{S}\,\text{sgn}(\mathbf{s}) \tag{16}$$

Substituting (16) into (15) yields

$$\begin{aligned}\dot{\mathbf{V}} &= -\mathbf{S}\hat{\mathbf{\Psi}}\,\text{sgn}(\mathbf{s}) - \mathbf{S}\mathbf{p} - \mathbf{\Delta}^{-1}(\mathbf{\Psi} - \hat{\mathbf{\Psi}})\mathbf{\Delta}\mathbf{S}\,\text{sgn}(\mathbf{s}) \\ &= -\mathbf{S}\hat{\mathbf{\Psi}}\,\text{sgn}(\mathbf{s}) - \mathbf{S}\mathbf{p} - \mathbf{\Delta}^{-1}\mathbf{\Psi}\mathbf{\Delta}\mathbf{S}\,\text{sgn}(\mathbf{s}) + \mathbf{\Delta}^{-1}\hat{\mathbf{\Psi}}\mathbf{\Delta}\mathbf{S}\,\text{sgn}(\mathbf{s})\end{aligned} \tag{17}$$

Because $\mathbf{S}$, $\mathbf{\Psi}$, $\widehat{\mathbf{\Psi}}$, and $\mathbf{\Delta}$ are diagonal matrices, they satisfy the commutative property of matrix multiplication. Thus,

$$\begin{aligned}\dot{\mathbf{V}} &= -\mathbf{S}\hat{\mathbf{\Psi}}\,\text{sgn}(\mathbf{s}) - \mathbf{S}\mathbf{p} - \mathbf{\Psi}\mathbf{S}\,\text{sgn}(\mathbf{s}) + \hat{\mathbf{\Psi}}\mathbf{S}\,\text{sgn}(\mathbf{s}) \\ &= -\mathbf{S}\mathbf{p} - \mathbf{\Psi}\mathbf{S}\,\text{sgn}(\mathbf{s})\end{aligned} \tag{18}$$

Considering the ith element of vector $\dot{\mathbf{V}}$ is

$$\begin{aligned}\dot{V}_i &= -s_i p_i - \psi_i s_i\,\text{sgn}(s_i) \\ &= -s_i p_i - \psi_i |s_i| \\ &\le |s_i||p_i| - \psi_i |s_i| \le (|p_i| - \psi_i)|s_i| \le 0\end{aligned} \tag{19}$$

The equation (19) shows that the stability of the proposed adaptive sliding mode control system is guaranteed. The convergence to zero of adaptation error $\tilde{\psi}_i$, sliding variable s_i are verified by the Lyapunov criterion. Hence, tracking error e_i converges to zero within finite time.

4. Case study: A 6-DOF industrial robot

The efficiency of the proposed adaptive sliding mode controller for a robot under actuator torque degradation is verified through an application example. Let us consider the IRB 120 industrial robot (a 6-DOF serial robot) made by ABB Robotics [23]. The initial configuration with attached-body frames and D-H parameters are depicted in Fig. 1 and Table 1, respectively.

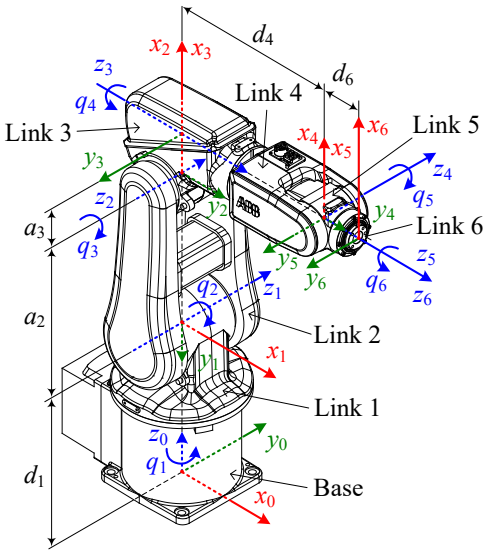

Fig. 1. The IRB 120 industrial robot with attached-body frames

Table 1

D-H parameters of the IRB 120 industrial robot

Joint i	θ_i (rad)	d_i (m)	a_i (m)	α_i (rad)
1	q_1	$d_1 = 0.29$	$a_1 = 0$	$\alpha_1 = -\pi/2$
2	$q_2 - \pi/2$	$d_2 = 0$	$a_2 = 0.27$	$\alpha_2 = 0$
3	q_3	$d_3 = 0$	$a_3 = 0.07$	$\alpha_3 = -\pi/2$
4	q_4	$d_4 = 0.302$	$a_4 = 0$	$\alpha_4 = \pi/2$
5	q_5	$d_5 = 0$	$a_5 = 0$	$\alpha_5 = -\pi/2$
6	q_6	$d_6 = 0.072$	$a_6 = 0$	$\alpha_6 = 0$

By adopting the robot dynamic formulation presented in [24], the generalized inertia matrix $\mathbf{M} \in \mathbb{R}^{6\times6}$ of the IRB 120 robot can be obtained as

$$\mathbf{M} = \sum_{i=1}^{6} \left(m_i (\mathbf{J}_{T_i}^0)^T \mathbf{J}_{T_i}^0 + \mathbf{J}_{R_i}^T \mathbf{I}_i \mathbf{J}_{R_i} \right) \tag{20}$$

The Coriolis/centrifugal matrix $\mathbf{C} \in \mathbb{R}^{6\times6}$ is

$$\mathbf{C} = \frac{1}{2} \left[\frac{\partial \mathbf{M}}{\partial \mathbf{q}} (\mathbf{1}_6 \otimes \dot{\mathbf{q}}) + \frac{\partial \mathbf{M}}{\partial \mathbf{q}} (\dot{\mathbf{q}} \otimes \mathbf{1}_6) - \left(\frac{\partial \mathbf{M}}{\partial \mathbf{q}} (\dot{\mathbf{q}} \otimes \mathbf{1}_6) \right)^T \right] \tag{21}$$

The vector of gravity term $\mathbf{g} \in \mathbb{R}^6$ is

$$\mathbf{g} = \left(\frac{\partial P}{\partial \mathbf{q}} \right)^T \tag{22}$$

where m_i is the mass of link i; $\mathbf{J}_{R_i}$, $\mathbf{J}_{T_i}^0 \in \mathbb{R}^{3\times 6}$ are the rotational and translational Jacobian matrices; $\mathbf{I}_i \in \mathbb{R}^{3\times 3}$ is the link inertia tensor with respect to the frame attached at the link centroid and parallel to the corresponding attached frame; $\mathbf{1}_6 \in \mathbb{R}^{6\times 6}$ is the identity matrix; $\otimes$ denotes Kronecker product operator; and P is the total potential energy. Based on the 3D CAD models of the IRB 120 robot links with data of their physical properties given by ABB Inc., the approximated values of mass m_i, link centroid $\mathbf{r}_{C_i}$ with respect to the corresponding attached coordinate, inertia tensor $\mathbf{I}_i$ can be achieved by a professional mechanical design software. The nominal robot parameters used in this paper are provided in [25] as follows:

$$\text{Base}: m_0 = 8.659$$

$$\text{Link } 1: m_1 = 4.248, \mathbf{r}_{C_1}^T = \begin{bmatrix} 0, & 54, & 0 \end{bmatrix} \times 10^{-3}, \mathbf{I}_1 = \begin{bmatrix} 19.699 & 0 & 0 \\ 0 & 14.484 & 0 \\ 0 & 0 & 19.952 \end{bmatrix} \times 10^{-3}$$

$$\text{Link } 2: m_2 = 5.412, \mathbf{r}_{C_2}^T = \begin{bmatrix} -169, & 0, & 0 \end{bmatrix} \times 10^{-3}, \mathbf{I}_2 = \begin{bmatrix} 35.942 & 0 & 0 \\ 0 & 83.522 & 0 \\ 0 & 0 & 57.569 \end{bmatrix} \times 10^{-3}$$

$$\text{Link } 3: m_3 = 4.077, \mathbf{r}_{C_3}^T = \begin{bmatrix} -12, & 0, & 23 \end{bmatrix} \times 10^{-3}, \mathbf{I}_3 = \begin{bmatrix} 17.562 & 0 & -1.993 \\ 0 & 23.140 & 0 \\ -1.993 & 0 & 11.589 \end{bmatrix} \times 10^{-3}$$

$$\text{Link } 4: m_4 = 1.832, \mathbf{r}_{C_4}^T = \begin{bmatrix} 0, & -7, & 0 \end{bmatrix} \times 10^{-3}, \mathbf{I}_4 = \begin{bmatrix} 7.247 & 0 & 0 \\ 0 & 3.919 & 0 \\ 0 & 0 & 5.551 \end{bmatrix} \times 10^{-3}$$

$$\text{Link } 5: m_5 = 0.755, \mathbf{r}_{C_5}^T = \begin{bmatrix} 0, & 0, & 0 \end{bmatrix}, \mathbf{I}_5 = \begin{bmatrix} 1.120 & 0 & 0 \\ 0 & 1.227 & 0 \\ 0 & 0 & 0.559 \end{bmatrix} \times 10^{-3}$$

$$\text{Link } 6: m_6 = 0.019, \mathbf{r}_{C_6}^T = \begin{bmatrix} 0, & 0, & -7 \end{bmatrix} \times 10^{-3}, \mathbf{I}_6 = \begin{bmatrix} 2.347 & 0 & 0 \\ 0 & 2.347 & 0 \\ 0 & 0 & 4.123 \end{bmatrix} \times 10^{-6} \quad (23)$$

where the units of mass, length, inertia tensor are kg, m, and kgm^2, respectively. The gravitational acceleration is 9.807m/s^2. The robot parameters are considered to be uncertain. Therefore, the control system uses the nominal values of robot parameters whereas the virtual robot (the control process model) is set up by Simscape Multibody with an error of 10% in all parameters.

For simulations, the robot's initial configuration is selected as $\mathbf{q}(0) = \dot{\mathbf{q}}(0) = [0, 0, 0, 0, 0, 0]^T$. The desired joint trajectory $\mathbf{q}_d = [q_{1d}, q_{2d}, \dots, q_{6d}]^T$ is given by

$$\begin{aligned} q_{1d} &= 2\sin(\pi t), & q_{4d} &= 2.5\sin(\pi t), \\ q_{2d} &= 1.5\sin(\pi t), & q_{5d} &= 2\sin(\pi t), \\ q_{3d} &= \sin(\pi t), & q_{6d} &= 3\sin(\pi t) \end{aligned} \quad (24)$$

The robot will be subject to PDT faults in two cases of torque degradation coefficient $\boldsymbol{\varphi}$. The small degradation case (case 1): $\boldsymbol{\varphi} = [0.9, 0.9, 0.9, 0.9, 0.9, 0.9]^T$ corresponds to 10% loss of PDT in every actuator; and the bad degradation case (case 2): $\boldsymbol{\varphi} = [0.5, 0.8, 0.8, 0.5, 0.5, 0.5]^T$ corresponds to 50% loss in actuator 1, 4, 5, 6, and 20% loss in actuator 2, 3. For performance comparison in each case with the same robot's parameters, several simulations are implemented in turn with two schemes: a conventional sliding mode control law (SMC), and the proposed adaptive sliding mode control law (ASMC). The conventional SMC with the same sliding manifold (6) is

$$\boldsymbol{\tau}_c = \mathbf{M}(\ddot{\mathbf{q}}_d + \mathbf{A}\dot{\mathbf{e}} + \mathbf{K}\text{sgn}(\mathbf{s})) + \mathbf{C}\dot{\mathbf{q}} + \mathbf{g} \quad (25)$$

where $\mathbf{K} = \text{diag}(\mathbf{k}) \in \mathbb{R}^{6\times 6}$ with $\mathbf{k} = [k_1, k_2, \dots, k_6]^T$, $k_i > 0$ $(i = 1, 2, \dots, 6)$; and the sliding condition is

$$\dot{\mathbf{s}} = -\mathbf{K}\text{sgn}(\mathbf{s}) \quad (26)$$

To reduce the chattering amplitude of sliding mode control system, saturation function sat(s_i/a_i) described in (27) can be used instead of sign function sgn(s_i) for both mentioned controllers.

$$\text{sat}(s_i/a_i) = \begin{cases} -1 & \text{if } s_i \le -a_i \\ (s_i/a_i) & \text{if } -a_i < s_i < a_i \\ 1 & \text{if } s_i \ge a_i \end{cases} \quad (27)$$

The parameters of the conventional SMC are selected as: sliding manifolds with $\alpha_1 = \alpha_2 = \alpha_3 = \alpha_4 = \alpha_5 = \alpha_6 = 15$; saturation functions with $a_1 = a_2 = a_3 = a_4 = a_5 = a_6 = 0.2$; gains $k_1 = k_2 = k_3 = k_4 = k_5 = k_6 = 30$. The proposed ASMC with the same sliding manifolds and saturation functions of

SMC is used, and its remaining parameters are chosen as: adaptation speed coefficients $\delta_1 = \delta_2 = \delta_3 = \delta_4 = \delta_5 = \delta_6 = 300$. Firstly, the robot system is simulated in the normal case (fault-free case) for both the conventional SMC and the proposed ASMC. Secondly, the two mentioned cases are implemented in turn for both control schemes. All simulations are conducted by MATLAB/Simulink and Simscape Toolbox with solver ode14x and the sample time of 0.001s. The system performances in the normal case, case 1, and case 2 are depicted in (Fig. 2, Fig. 3), (Fig. 4 - Fig. 7), and (Fig. 8 - Fig. 11), respectively.

In the normal case, Fig. 2 and Fig. 3 show that both the conventional SMC and the designed ASMC give good and similar performances. The robot joints match the desired trajectories after about 0.5s.

In case 1 (10% loss of PDT faults in all actuators):

Control torque and actuator torque of the robot when using the SMC and the ASMC are depicted in Fig. 6 and Fig. 7, respectively. The fault actuators can only provide 90% of the required control torque. After the time that the robot responses can follow the references, the control torque in Fig. 6 and Fig. 7 may appear to be almost similar in shape. However, in the transient time, the control torque of ASMC (Fig. 7) changes more quickly than that of SMC (Fig. 6). Consequently, tracking error $\mathbf{e}_{\mathrm{ASMC}}$ is smaller and converges faster than $\mathbf{e}_{\mathrm{SMC}}$ (Fig. 5). Under effects of 10% loss of PDT faults in all actuators, Fig. 4 and Fig. 5 indicate that the robot joint responses when using the SMC start to deviate from the desired trajectories with the maximum tracking error in joint 5 ($e_{5\,\mathrm{SMC}}$ oscillating in [-0.01, 0.01]) and the minimum tracking error in joint 1, joint 2 ($e_{1\,\mathrm{SMC}}$, $e_{2\,\mathrm{SMC}}$ oscillating in the same range [-0.005, 0.005]); whereas the proposed ASMC gives better joint responses with tracking errors varying in the much smaller bounds.

In case 2 (50% loss of PDT faults in actuator 1, 4, 5, 6, and 20% loss in actuator 2, 3):

When the percentage of actuator torque loss increases to 50% in actuator 1, 4, 5, 6, and 20% in actuator 2, 3 (Fig. 10 and Fig. 11 for the SMC and the ASMC, respectively), the control torque generated by the ASMC and SMC is quite different, especially at actuator 1, 4, 5, and 6. The robot performance using the SMC becomes significantly worse with large tracking errors in most joints (Fig. 9). As manifested in Fig. 8, some joint angles cannot follow the desired trajectories when the SMC is used, i.e., joint 1, 4, 5, and 6. Meanwhile, by using the proposed ASMC, the joint responses still track the desired paths with acceptable tracking errors fluctuating in the range of [-0.005, 0.005] for all joints.

Compared with a SMC scheme, it is obvious that the better joint responses can be achieved by using the proposed ASMC despite the existence of PDT faults in actuators. In other words, the proposed ASMC methodology can tolerate the PDT fault problem in a serial robot system.

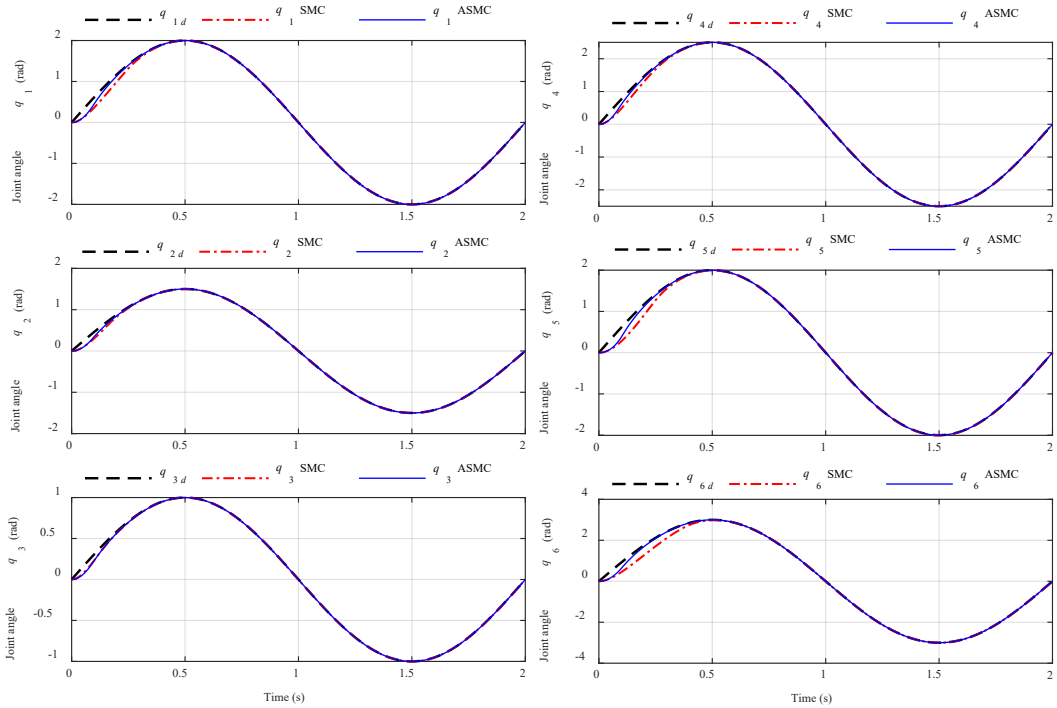

Fig. 2. References and responses of the IRB 120 robot using SMC and ASMC in the normal case

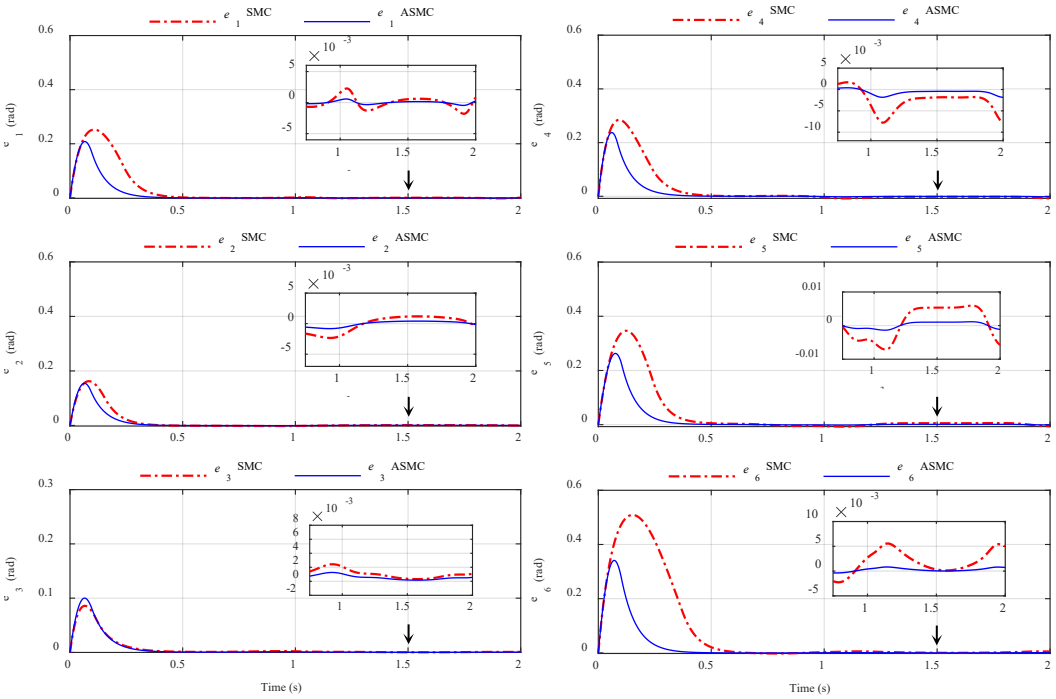

Fig. 3. Tracking errors of the IRB 120 robot using SMC and ASMC in the normal case

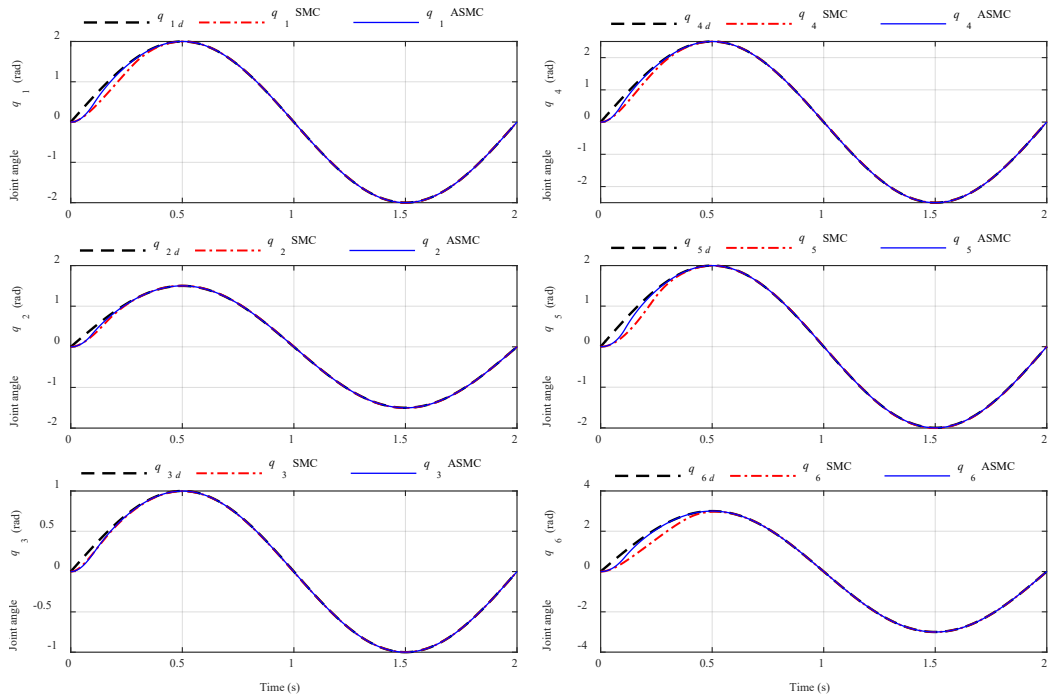

Fig. 4. References and responses of the IRB 120 robot using SMC and ASMC under PDT faults of 10% loss in all actuators (case 1)

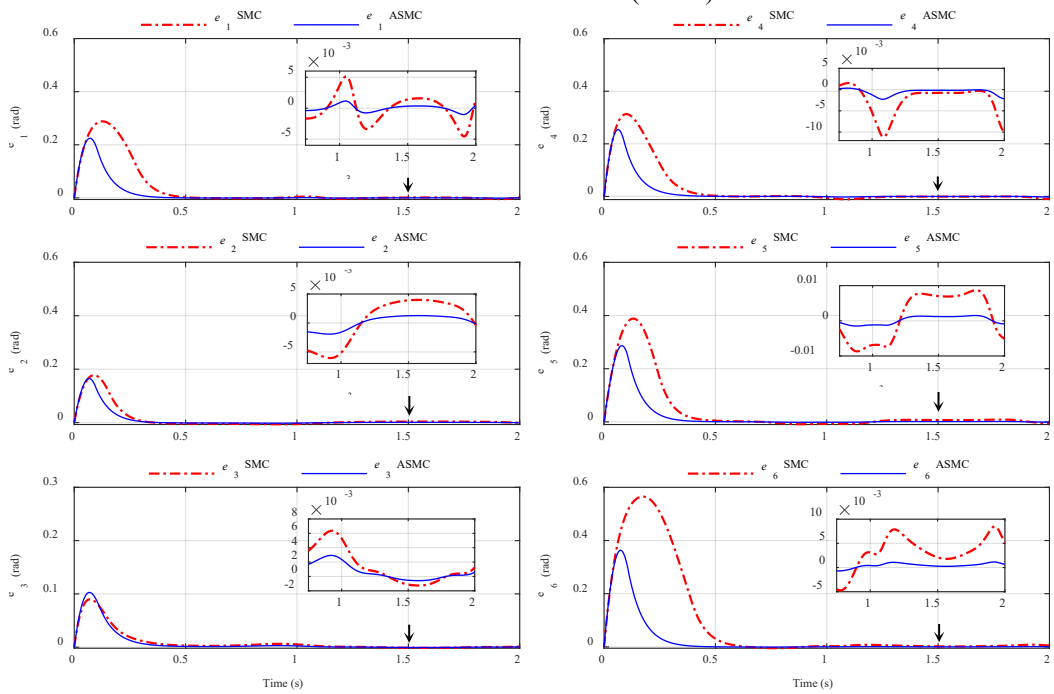

Fig. 5. Tracking errors of the IRB 120 robot using SMC and ASMC under PDT faults of 10% loss in all actuators (case 1)

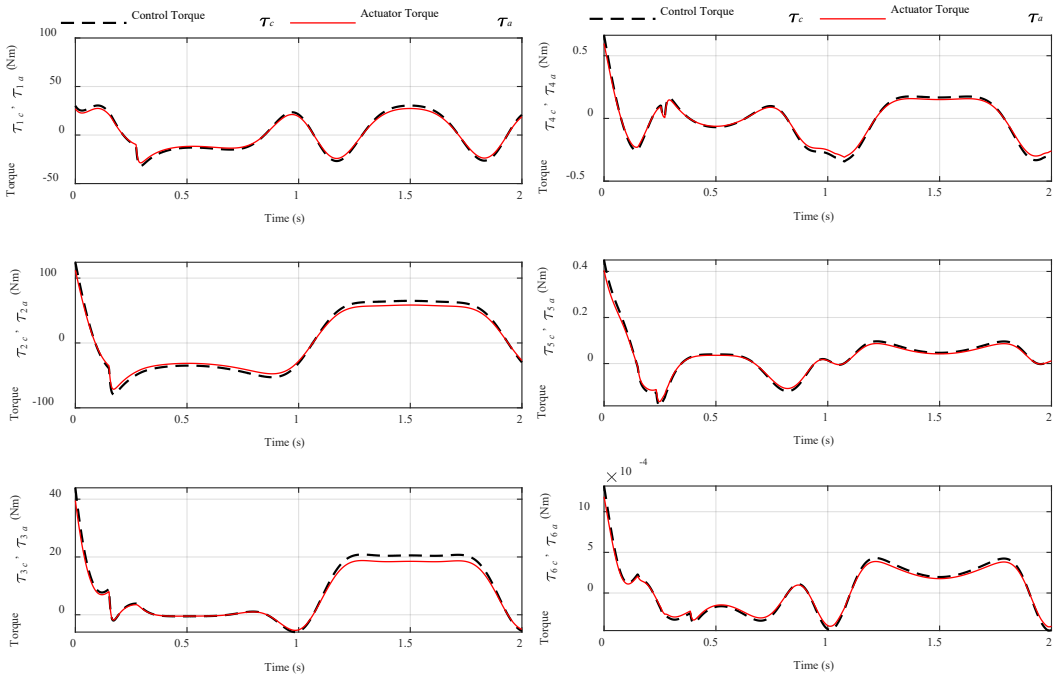

Fig. 6. Control torque and actuator torque of the IRB 120 robot using SMC under PDT faults of 10% loss in all actuators (case 1)

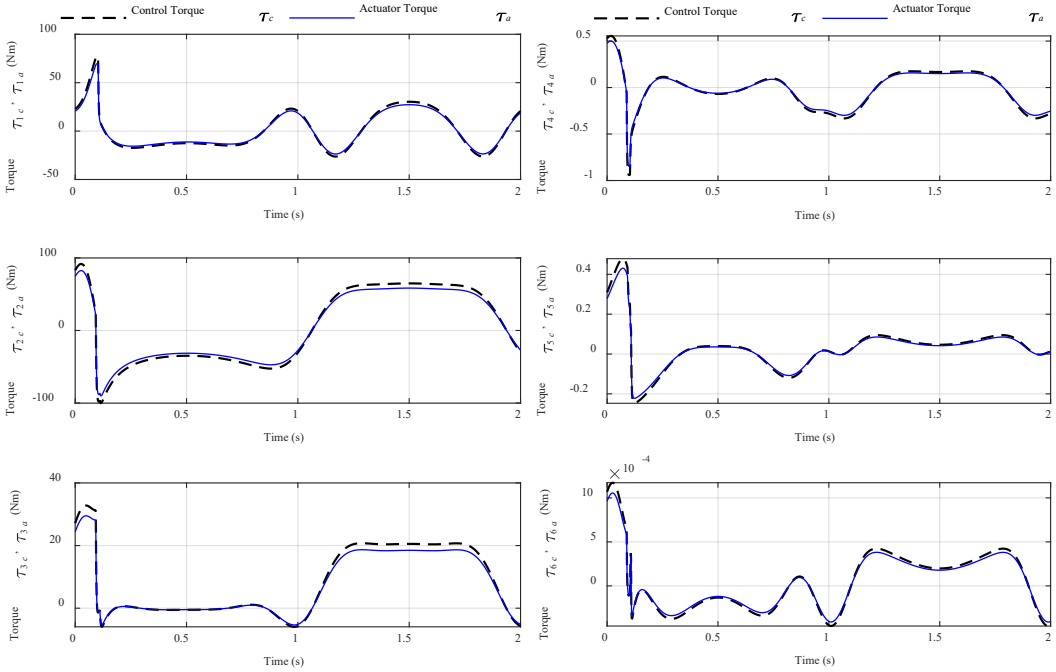

Fig. 7. Control torque and actuator torque of the IRB 120 robot using ASMC under PDT faults of 10% loss in all actuators (case 1)

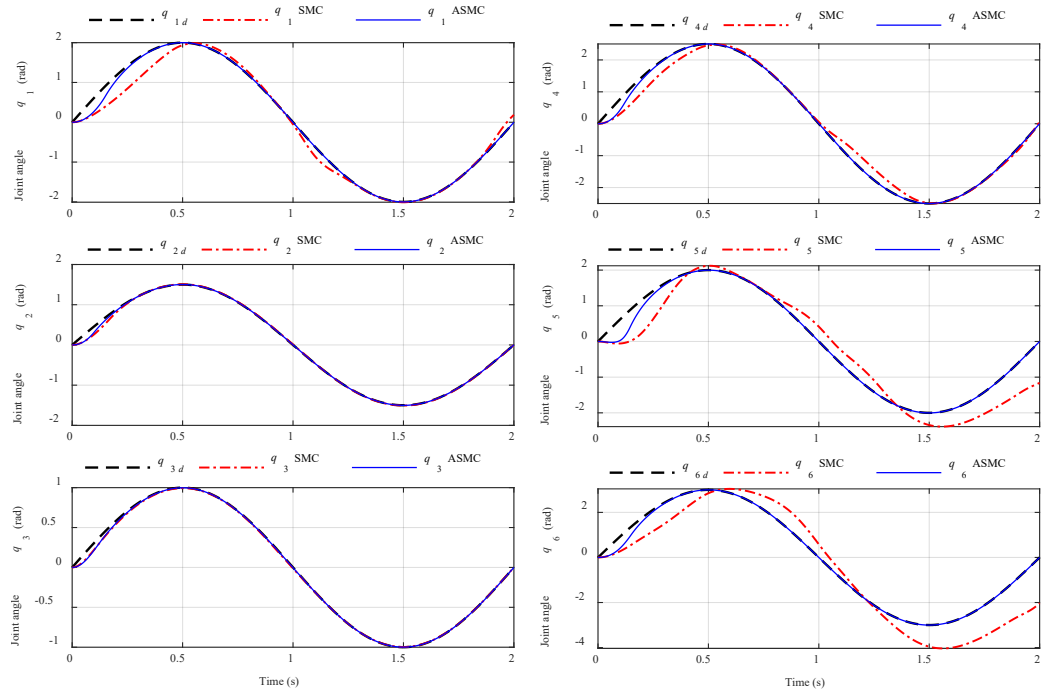

Fig. 8. References and responses of the IRB 120 robot using SMC and ASMC under PDT faults of 50% loss in actuator 1,4,5,6, and 20% loss in actuator 2, 3 (case 2)

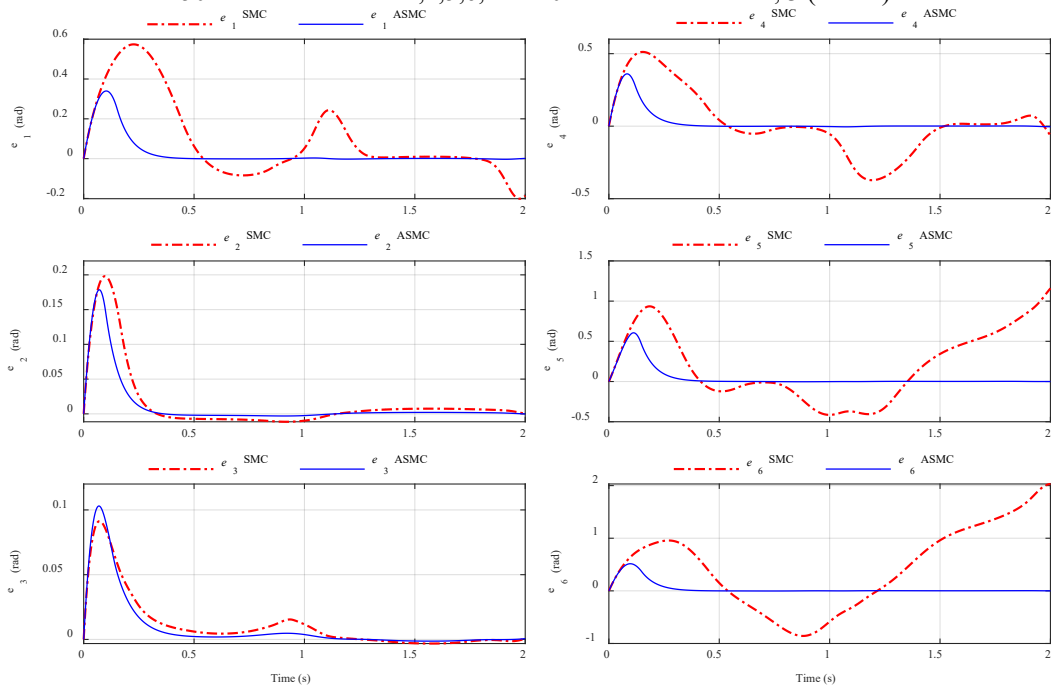

Fig. 9. Tracking errors of the IRB 120 robot using SMC and ASMC under PDT faults of 50% loss in actuator 1, 4, 5, 6, and 20% loss in actuator 2, 3 (case 2)

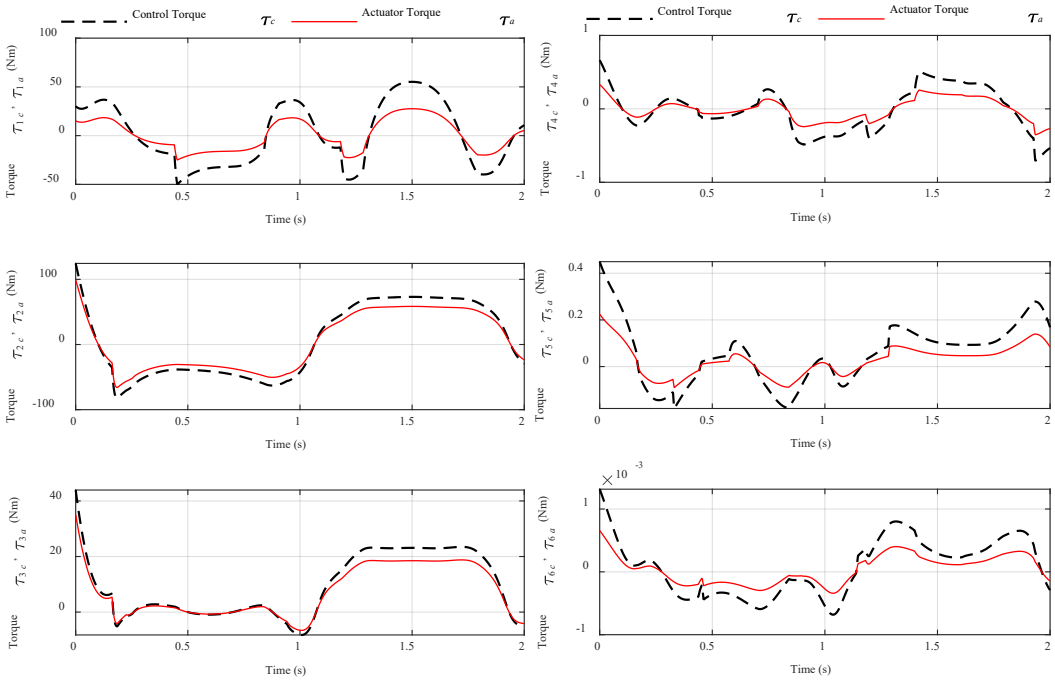

Fig. 10. Control and actuator torque of the IRB 120 robot using SMC under PDT faults of 50% loss in actuator 1,4,5,6, and 20% loss in actuator 2, 3 (case 2)

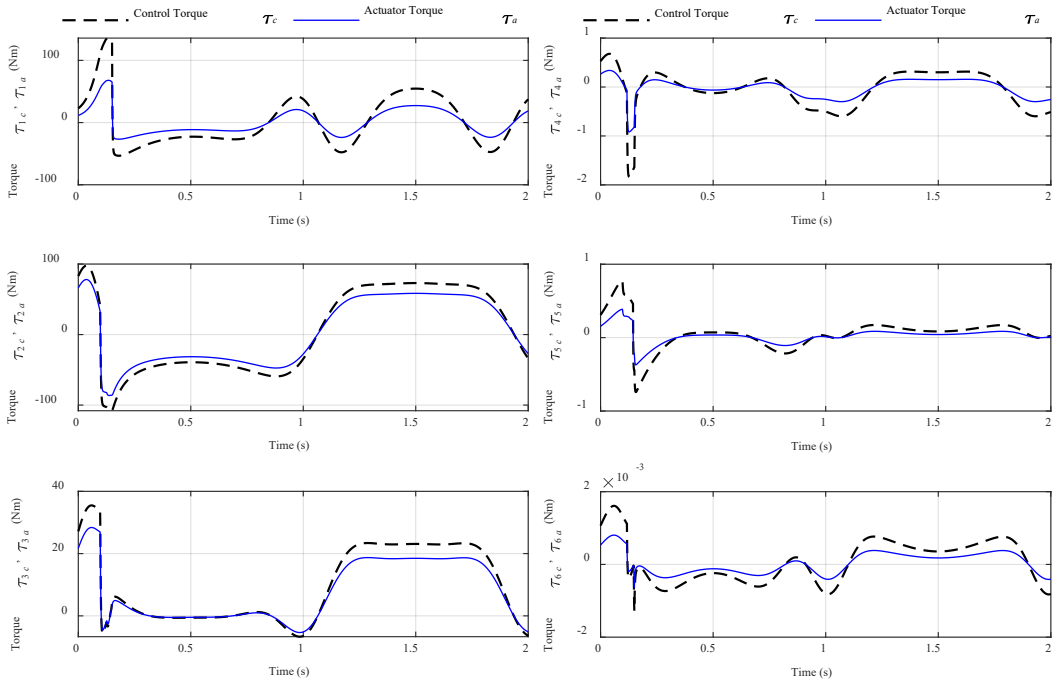

Fig. 11. Control and actuator torque of the IRB 120 robot using ASMC under PDT faults of 50% loss in actuator 1,4,5,6, and 20% loss in actuator 2, 3 (case 2)

5. Conclusions

The paper deals with the design of robot controllers in presence of actuator faults and uncertain parameters. The actuator fault type considered in this investigation is proportional degradation of torque. An adaptive sliding mode controller is synthesized for a serial robot with ability to tolerate the mentioned fault. The system stability is guaranteed by the Lyapunov method in the control design procedure. The effectiveness of the proposed controller is verified by an application for a 6-DOF serial robot. The simulation results, compared with a conventional sliding mode control, demonstrate that the fault-tolerant capability of the proposed ASMC is considerably better than that of the conventional SMC. In case of using the proposed ASMC, the robot can follow the desired trajectories with sufficiently small errors if the percentage of torque loss is up to about 10% in all actuators. The greater the torque loss, the worse the tracking error; the proposed ASMC still gives acceptable performance even if the torque loss increases up to 50% by some actuators. However, external disturbances have not been considered and will be addressed in a future study.

Acknowledgements

This research is supported by Vingroup Innovation Foundation (VINIF) in project code VINIF.2020.NCUD.DA059.

REFERENCES

[1]. *Z. Tie, L. X. Hong, K. Z. Qiang, and G. W. Tao*, "Real-time feedforward torque control of an industrial robot based on the dynamics model", UPB Sci. Bull. Ser. D Mech. Eng., **vol. 82**, no. 1, pp. 3–18, 2020.

[2]. *X. Xiaofei, Y. Shuhui, and L. Denghua*, "Modeling and analysing for writing robot arm", UPB Sci. Bull. Ser. D Mech. Eng., **vol. 80**, no. 1, pp. 3–16, 2018.

[3]. *V. Sathish, S. Ramaswamy, and S. Butail*, "Training data selection criteria for detecting failures in industrial robots", IFAC-PapersOnLine, **vol. 49**, no. 1, pp. 385–390, 2016.

[4]. *F. Caccavale, P. Cilibrizzi, F. Pierri, and L. Villani*, "Actuators fault diagnosis for robot manipulators with uncertain model", Control Eng. Pract., **vol. 17**, no. 1, pp. 146–157, 2009.

[5]. *R. Muradore and P. Fiorini*, "A PLS-based statistical approach for fault detection and isolation of robotic manipulators", IEEE Trans. Ind. Electron., **vol. 59**, no. 8, pp. 3167–3175, 2012.

[6]. *M. L. McIntyre, W. E. Dixon, D. M. Dawson, and I. D. Walker*, "Fault identification for robot manipulators", IEEE Trans. Robot., **vol. 21**, no. 5, pp. 1028–1034, 2005.

[7]. *A. De Luca and R. Mattone*, "An identification scheme for robot actuator faults", in IEEE/RSJ International Conference on Intelligent Robots and Systems, 2005, pp. 2613–2617.

[8]. *F. Caccavale, A. Marino, G. Muscio, and F. Pierri*, "Discrete-time framework for fault diagnosis in robotic manipulators", IEEE Trans. Control Syst. Technol., **vol. 21**, no. 5, pp. 1858–1873, 2013.

[9]. *Y. Zeng, Y.-R. Xing, H.-J. Ma, and G.-H. Yang*, "Adaptive fault diagnosis for robot manipulators with multiple actuator and sensor faults", in 27th Chinese Control and Decision Conference (CCDC), 2015, pp. 6569–6574.
[10]. *W. Domski and A. Mazur*, "Emergency control of a space 3R manipulator in case of one joint failure", in 2017 22nd International Conference on Methods and Models in Automation and Robotics (MMAR), 2017, pp. 384–389.
[11]. *Z. Mu, L. Han, W. Xu, B. Li, and B. Liang*, "Kinematic analysis and fault-tolerant trajectory planning of space manipulator under a single joint failure", Robot. Biomimetics, **vol. 3**, no. 16, 2016.
[12]. *L. N. Truc, N. T. Nghia, N. T. Thanh, N. M. Thien, and T. L. Nguyen*, "Effect of Actuator Torque Degradation on Behavior of a 6-DOF Industrial Robot", Univers. J. Mech. Eng., **vol. 8**, no. 2, pp. 114–128, 2020.
[13]. *G. Liu*, "Control of robot manipulators with consideration of actuator performance degradation and failures", in 2001 IEEE International Conference on Robotics & Automation, 2001, pp. 2566–2571.
[14]. *R. Lei and L. Chen*, "Adaptive fault-tolerant control based on boundary estimation for space robot under joint actuator faults and uncertain parameters", Def. Technol., **vol. 15**, no. 6, pp. 964–971, 2019.
[15]. *X. Jin*, "Adaptive finite-time tracking control for joint position constrained robot manipulators with actuator faults", in American Control Conference, 2016, pp. 6018–6023.
[16]. *V. G. Adîr, A. M. Stoica, and J. F. Whidborne*, "Sliding mode control of a 4Y octorotor", UPB Sci. Bull. Ser. D Mech. Eng., **vol. 74**, no. 4, pp. 37–52, 2012.
[17]. *L. Laggoun, L. Youb, B. Sebti, S. Benaggoune, and A. Craciunescu*, "Direct Torque Control Using Second Order Sliding Mode of a Double Star Permanent Magnet Synchronous Machine", UPB Sci. Bull. Ser. C Electr. Eng. Comput. Sci., **vol. 80**, no. 4, pp. 93–106, 2018.
[18]. *B. Xiao and S. Yin*, "An fast reconstruction approach for actuator fault in robot manipulators", in 2016 14th International Workshop on Variable Structure Systems (VSS), 2016, pp. 414–419.
[19]. *A. Freddi, S. Longhi, A. Monteriù, D. Ortenzi, and D. Proietti Pagnotta*, "Fault Tolerant Control Scheme for Robotic Manipulators Affected by Torque Faults", IFAC-PapersOnLine, **vol. 51**, no. 24, pp. 886–893, 2018.
[20]. *S. J. Yoo*, "Actuator fault detection and adaptive accommodation control of flexible-joint robots", IET Control Theory Appl., **vol. 6**, no. 10, pp. 1497–1507, 2012.
[21]. *J.-H. Shin and J.-J. Lee*, "Fault detection and robust fault recovery control for robot manipulators with actuator failures", in 1999 IEEE International Conference on Robotics and Automation, 1999, pp. 861–866.
[22]. *Y. She, W. Xu, H. Su, B. Liang, and H. Shi*, "Fault-tolerant analysis and control of SSRMS-type manipulators with single-joint failure", Acta Astronaut., **vol. 120**, pp. 270–286, 2016.
[23]. "Product specification IRB 120 (Document ID: 3HAC035960-001)", ABB Robotics, 2018.
[24]. *L. N. Truc, N. V. Quyen, and N. P. Quang*, "Dynamic model with a new formulation of Coriolis/centrifugal matrix for robot manipulators", J. Comput. Sci. Cybern., **vol. 36**, no. 1, pp. 89–104, 2020.
[25]. *L. N. Truc and N. T. Lam*, "Quasi-physical modeling of robot IRB 120 using Simscape Multibody for dynamic and control simulation", Turkish J. Electr. Eng. Comput. Sci., **vol. 28**, no. 4, pp. 1949–1964, 2020.